Proceedings of The Fifteenth (2005) International Offshore and Polar Engineering Conference
Seoul, Korea, June 19–24, 2005

ISBN 1-880653-64-8 (Set); ISSN 1098-6189 (Set)

Simulation of Dynamic Loading in Centrifuge Modeling for Suction Bucket Foundations

Xiaobin Lu[1], Jianhong Zhang[2], Guoliang Sun[2], Zuyu Chen[2]

1 Institute of Mechanics, China Academy of Science, Beijing, China
2 Department of Hydraulic Engineering, Tsinghua University, Beijing, China

ABSTRACT

Suction bucket foundations are widely used in the offshore platform for the exploitation of the offshore petroleum and natural gas resources in the Bohai Bay of China. During winter seasons, ice sheets formed in Bohai Bay will impose strong impact and result in strong vibration on the platform. The measured frequency of the structural vibration of the platforms is 0.8~1.0 Hz. This paper describes a dynamic loading device developed on the geotechnical centrifuge at Tsinghua University and its application in modeling suction bucket foundation under the equivalent ice-induced vibration loadings.

KEY WORDS: Suction bucket foundation; dynamic loading device; ice-sheet; vibration; centrifuge modeling; pore water pressure.

INTRODUCTION

The suction bucket is a large diameter cylinder, which is closed at the top and open at the bottom. Pump inlets and relief valves are mounted at the top. The cylinder is lowered to the sea floor under its own weight, with the relief valves open. After a sufficient penetration into the soil, the pump is started to generate differential pressure which drives the bucket into the soil at a required penetration depth. The pump and relief valves will be retrieved after installation. Experience shows that the application of the suction foundation in up to 3000 m of water would be possible.

The Suction installed bucket foundations are more and more commonly used for a variety of offshore structures. This type of foundation is beneficial both during installation and under extreme horizontal and moment loadings. It also has been gradually used as the foundation of the offshore platform in the exploitation of the offshore petroleum and natural gas resources in Bohai bay of China, as shown in Fig. 1. However, during winter seasons, ice sheets formed in the Bohai Bay will impose strong impact and result in serious vibration on the platform. The measured frequency of the structural vibration of the platforms is 0.8~1.0 Hz. In order to investigate the dynamic response of the suction bucket foundations and the surrounding soils, centrifuge tests have been performed on the 50 g-t geotechncal centrifuge at Tsinghua University, Beijing, China. A dynamic loading device comprised primarily of an electromagnetic actuator has been developed by the Institute of Mechanics, China Academy of Science and Tsinghua University.

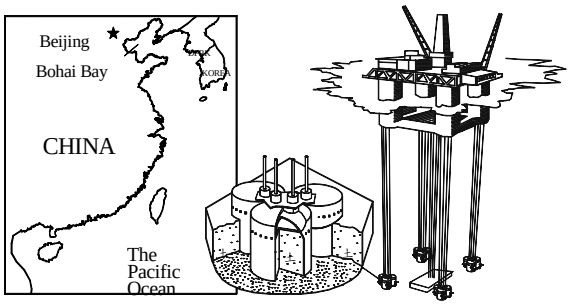

Fig. 1 Location of Bohai Bay

Modeling suction piles by centrifuges has been investigated by a number of researchers (Fuglsang et al. 1991; Renzi et al. 1991; Clukey and Morrison 1993; Clukey et al.1995; Watson and Randolph 1997; Allersma et al. 1997, 1999, 2001, 2003; Cao 2003). It has the advantages of properly modeling body forces and being capable of performing multiple tests at reduced costs. However, dynamic loadings with a large number of cycles are also an important feature of loadings encountered in the offshore environment. In dynamic centrifuge modeling, the inertial effect requires that the frequency and the amplitude of the horizontal force are scaled by N and $1/N^2$ respectively where N is the geometric as well as the gravity scale factor. Cyclic loading devices have been developed historically. Craig (1981) and Hjortnaes-Pedersen and Nelissen (1991) described a system that can produce high frequency dynamic loading of up to 10 Hz and 300 Hz on shallow foundations. Tan (1990) used pneumatic jacks controlled by a system of solenoid waves and timing mechanism to apply one directional loading to a single spudcan model. The highest frequency of the load is 1Hz. Dean et al. (1993) used an electrically operated servo-motor to drive a central threaded carriage back and forwarth to produce horizontal cyclic force, with a frequency of up to 3 Hz, on a 3-leg jack-up model. Ng et al. (1994) developed a servo controlled electro-hydraulic loading system for shallow foundations, the excitation frequency ranges between 0.1Hz to 10 Hz. Zhang et al. (2003) developed an electro-magnetic actuator and described its preliminary applications

This paper describes this dynamic loading device on centrifuge and presents some results of the centrifuge tests on suction bucket foundation under horizontal cyclic loading.

DYNAMIC LOADING DEVICE

The dynamic loading device is composed primarily of an electro-magnetic actuator as shown in Fig. 2. This actuator consists of a permanent magnet, a cylindrical silver coil, two copper disk springs, a load cell and a steel rod connected to the coil. There are two main technical challenges associated with the design of the actuator. (1) The cylindrical coil is suspended in a prefabricated space in the permanent magnet. The space is very tiny in order to avoid magnetic loss. However, since this cylindrical coil moves horizontally, it is orthogonal to the gravitational force, the deformation of the coil under this gravity lock it in this tiny space. In order to prevent this situation a linear bearing and two disk springs are installed to make the coil move linearly. This technique has been demonstrated to be very effective. (2) The weight of the coil should be minimized to reduce its deformation in the direction of centrifugal acceleration. Silver wire is used to form the cylindrical coil so as to enhance the performance and limit the weight within 0.5 kg. The total weight of the device is 14 kg. Consequently, the vibration of the 0.5 kg coil would not impose significant impact on the strong box whose weight is 150 kg. The coil moves back and forth, applying cyclic loading on the model bucket through a rigid rod.

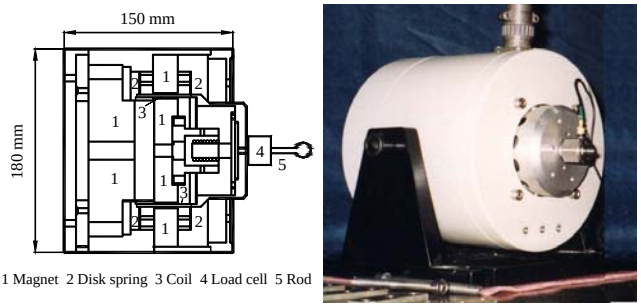

(a) Schematic diagram (b) Picture

Fig. 2 The electro-magnetic actuator

Fig. 3 is the controlling system for the loading device. The loading function is fed from a computer signal generator into a servo amplifier. The latter in turn generates the necessary electrical signals to control the intensity of electric current in the actuator. The output from the actuator in the form of load is continuously monitored by the load cell and fed back through a charged amplifier to the oscillograph. The load-electricity performance has been calibrated, which will be described in latter sections. Output signal from pore pressure transducer (PPT) and linear variable displacement transformers (LVDT) were passed across the centrifuge slipring and converted to digital data.

Table 1. Technical specification of the electromagnetic actuator

Diameter (mm)	Length (mm)	Weight (kg)	Frequency range (Hz)	Peak cyclic load (N)
180	260	14	1-120	100

With this device, the amplitude and the frequency of a horizontal cyclic force is reproduced at centrifugal acceleration of 80 g. Therefore in the centrifuge, the peak cyclic loading of 100 N and 64 Hz represents a prototype loading of 640 KN and 0.8 Hz for a single bucket foundation. Table 1 shows the technical specifications of this actuator.

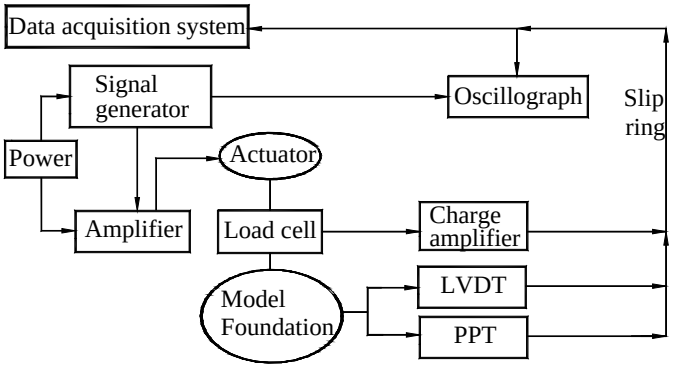

Fig.3 Controlling system of the loading device

PERFORMANCE OF THE LOADING DEVICE AT 1 G

Performance tests were conducted at 1 g condition to evaluate the frequency response of the loading system. Due to the low soil strength under 1 g condition, these tests cannot be carried out on the original soil foundation without causing a bearing capacity failure. As a result, the load was applied onto a rigid steel beam. A rubber pad was placed between the rod of the actuator and the steel beam. Sinusoidal loading functions with frequency ranging between 10 Hz and 120 Hz were used. The feedback from the load cell was captured and compared with the command signal. The supply load was 50 kN. Fig. 4 shows the typical time history of loading and the frequency response. Table 2 summarizes the frequency response at 1 g condition. The amplitude ratio and the phase lag increase with frequency, as shown in Table 2. Nevertheless the shape of the input sinusoidal form is preserved.

Table 2. Frequency response at 1 g condition

Frequency (Hz)	Magnitude ratio (dB)	Phase lag (°)
10	0	-21.6
20	0.356	-24.2
30	-0.389	-12.6
40	-0.935	17.4
50	-1.454	36
60	-1.788	39
70	-2.133	42
80	-2.421	50
90	-2.595	52
100	-2.776	56.2
110	-2.869	60.6
120	-3.062	72.5

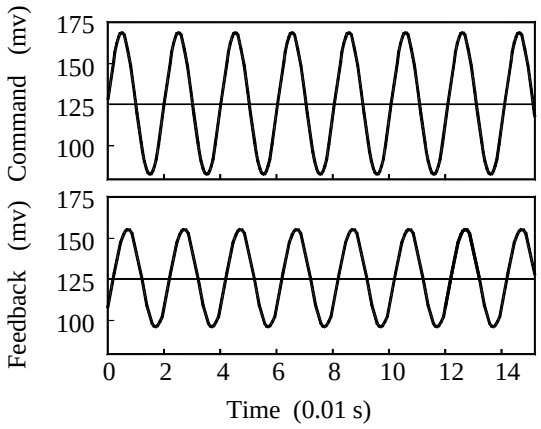

(a) Freq. = 50 Hz

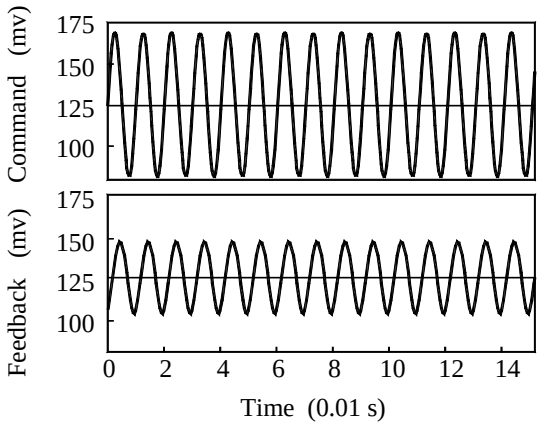

(b) Freq. = 100 Hz

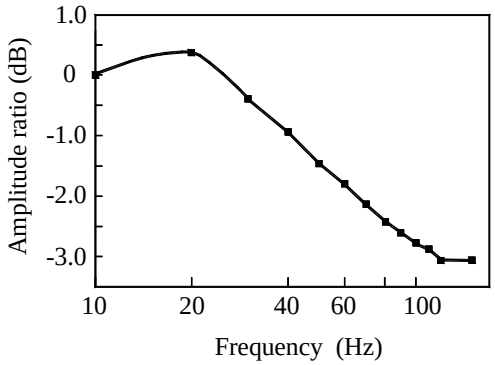

(c) Amplitude ratio

Fig. 4 Frequency response of the loading device at 1 g

THE CENTRIFUGE SYSTEM CONFIGURATION

Fig. 5 shows the configuration of the centrifuge and the model. Fig. 6 is a picture of the centrifuge model on the swing platform (camera absented). The internal area of the aluminum strong box measures 600 mm × 350 mm. The height of the strong box is also 350 mm. The thickness of the silty sand is 210 mm, underlain by 20 mm coarse sand. There is 20 mm high water above the soil surface. The actuator is supported by two steel beams fastened on the flange. Two rods fix the back of the actuator against the side of the strong box, as shown in Fig. 5. A miniature TV camera was attached to the flange of the model container to monitor the motion of the model bucket. The model bucket is a steel cylinder which has an external diameter of 60 mm, a thickness of 2 mm, and a height of 72 mm. A steel shaft connected to the bucket, which has a diameter of 8 mm. The dead weight of the platform was simulated by a ballast mounted on the top of the shaft. The movement of the bucket was monitored by two LVDTs. When the centrifuge model is tested under 80 g, its behavior would primarily correspond to that of a prototype footing with a diameter of 4.8 m.

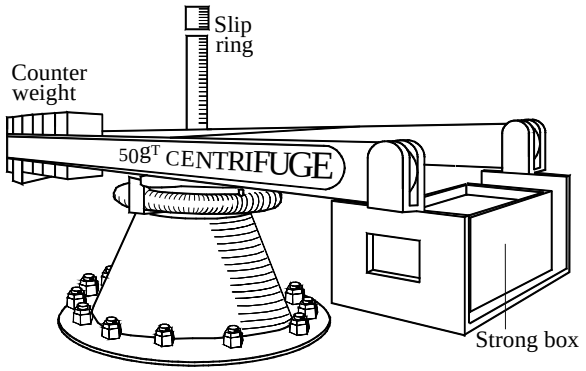

(a) 50 g-t centrifuge at Tsinghua University

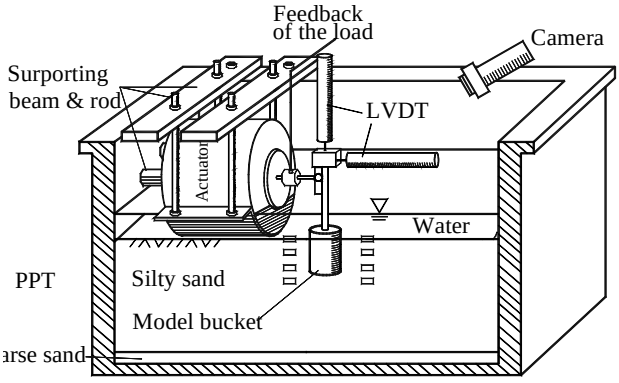

(b) Schematic diagram of centrifuge model

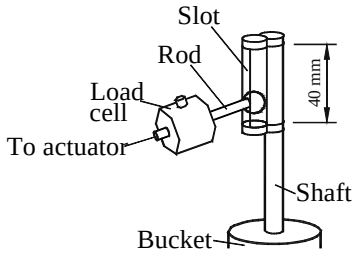

(c) Conncetion between the actuator and the bucket

Fig. 5 Configurations of the centrifuge and the model

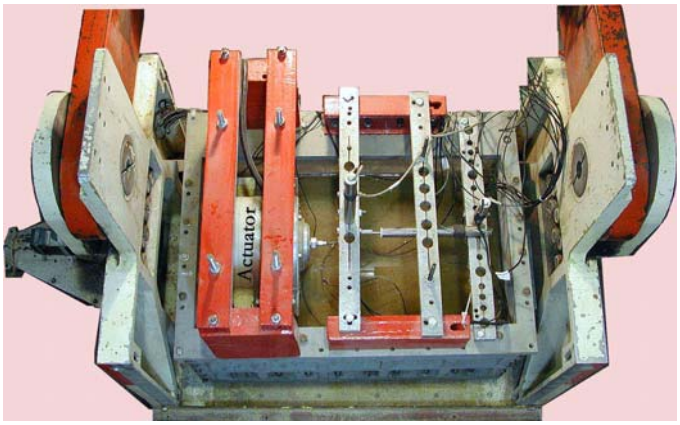

Fig. 6 The centrifuge model on the swing platform

PERFORMANCE OF THE LOADING DEVICE AT 80 G

Performance tests of the dynamic loading device were also carried out at 80 g. The actuator is connected with the model bucket through a rod with a steel ball at the end. This ball is 8 mm in diameter, which can slide vertically in a slot along the shaft. This slot is a steel pipe of 8 mm in diameter, with a 5 mm wide cut to facilitate the movement of the ball. Fig. 5c shows the detail of the connection. Therefore the force from the actuator was transferred to the bucket. However, bumping occurs due to the tiny gap between the ball and the slot, resulting in noise in the load function as shown in Fig. 7a. The shape is not so smooth as that at 1 g level, since the system excited is much complicated, including the actuator itself, the connection, the bucket foundation and the soil. Fig. 7b gives the relationship between the provided electric current and the output force.

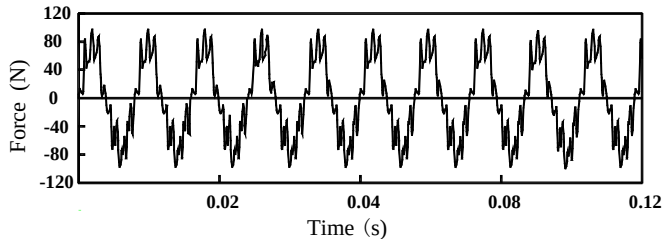

(a) Load function

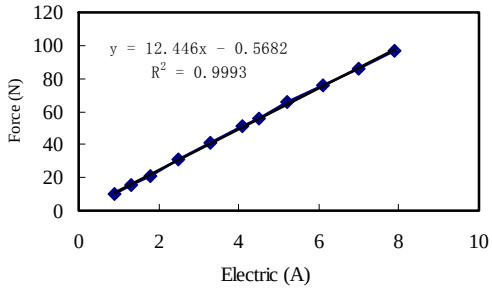

(b) Force-electric relation

Fig. 7 Load function at 80 g

Model Preparation

So far two approaches have been used to resolve the scale conflicts in dynamic centrifuge tests (Lee and schofield 1988, Kutter, et al. 1989). In this paper a finer soil was used so as to reduce the permeability (Kutter, et al. 1989). A medium silica sand was mixed with a silt to obtain a soil with lower permeability. Since the mixed soil has a 3.2 % clay content, so water was still used as the pore fluid. The reduction factor is about 40, less than 80 (the gravity scale factor). Therefore, the dissipation of pore water pressure should be faster than prototype thus may result in lower residual pore water pressure.

All soil samples were compacted by 5 layers, at a dry density of 1.52 g/cm^3. Pore water pressures transducers were embedded in the soil. The model was saturated by vacuum pumping to achieve saturation degrees over 97%. The soil model was consolidated at 80 g. After consolidation, the dry density of soil was measured to be 1.60 g/cm^3. The saturated permeability at the dry density of 1.60 g/cm^3 was measured to be $2*10^{-4}$ cm/s. Triaxial compression tests were also performed to obtain the consolidated drained shear strength, e.g. cohesion c = 0 kPa, effective internal friction angle $\varphi' = 35^o$. The properties of the soil are listed in Table 3.

Table 3. Properties of the soil

Classification	Silt
Specific gravity	2.69
Gradation	
0.074 mm < d <0.5 mm	81.49 %
0.005 mm < d <0.074 mm	15.3 %
d < 0.005 mm	3.2 %
Grain size	
D_{60}	0.15 mm
D_{10}	0.035 mm
Uniformity coefficient	4.28
Dry density	1.52 g/cm^3
Saturated permeability	$2*10^{-4}$ cm/s
Strength parameters	
Cohesion	0 kPa
Effective internal friction angle	35^o

Test Procedure

Centrifuge model was moved onto the platform of the centrifuge after the saturation of the soil. Static vertical load, 2048 kN in prototype scale, on the bucket was simulated by the weight of the model bucket plus a mass mounted on the shaft. The soil was consolidated under 80 g for 40 minutes (6 month in the prototype). LVDT recorded 1 cm consolidation settlement. Afterwards, the bucket was applied with a horizontal cyclic load for twenty minutes corresponding to a duration of 26.7 hours in the prototype. The actuator was load controlled. Output signal from the load cells, PPTs and LVDTs were passed across the centrifuge slipring and converted to digital data. During excitation, the shape of the load function remains unchanged. The magnitude of the load may decrease but not significantly.

RESULTS OF CENTRIFUGE TESTS

In this series of tests, the behavior of the bucket under horizontal cyclic loading is investigated, and the effect of the length of the bucket on the foundation response is also evaluated. This cyclic load has a peak of 60 N and a frequency of 64 Hz, which corresponds to a prototype load of 384 kN and 0.8 Hz. Two model buckets were adopted, having the same diameter of 60 mm but different lengths of 72 mm and 90 mm respectively. In order to facilitate the description, the centrifuge model, having the bucket of 72 mm in length, is designated Model 1, while the other one having the bucket of 90 mm in length is denoted by Model 2. The results of these two centrifuge models are described as follows.

Model 1

Fig. 8 shows the layout of eight pore water pressure transducers for Model 1, denoted by P1 ~ P8. The embedded depths of the transducers were calibrated in excavation of the model after the centrifuge testing and were transferred to prototype values as shown in Table 4.

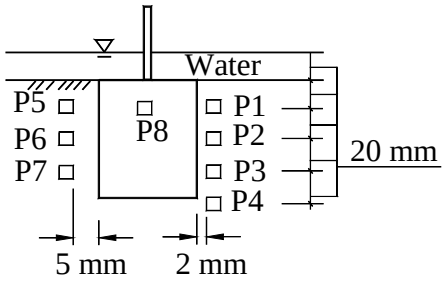

Fig. 8 Layout of the PPTs of No 1~8 for Model 1.

Fig. 9 shows the excess pore water pressure in Model 1 during excitation. Values in Fig. 9 are transferred to prototype scale. Figs. 9a and 9b show the excess pore pressure recorded by P1, P2, P3 and P4, and the pressure profiles 2 mm in horizontal from the side of the bucket. P1 indicates a high pore pressure region. The ratio of the maximum excess pore water pressure Δu_m, over the vertical effective stress σ_v' in the soil is approximately to be unity at P1, as shown in Table 4. Liquefaction potential may exist within a depth of 1.5 m. Also when centrifuge was stopped, fine soil particles were observed at the surface of the ground on the edge of the bucket. Since P1 is located near the surface, it also presents sharp variation, indicating fast dissipation of excess pore water pressure. However, P2, P3 and P4 didn't present significant peak values. They arrive at a steady state within about 5 hours. Both the maximum and residual excess pore pressure profiles, Δu_m and $\triangle u_r$, decrease with the soil depth, as shown in Fig. 9b. The profile curve presents the maximum pressure at P1, which sharply decreases to P2, and continuously decreases to P3 and P4.

Fig. 9c shows the excess pore pressure recorded by P5 and P7. P6 failed during the test. These two transducers were installed at 5 mm distance to the opposite side of the bucket. Similar to P1, P5, they also present distinct peaks. The ratio of $\Delta u_m/\sigma_v'$ at P5 is 0.94, being very close to unity. However, since it is located comparatively far from the bucket, the peak comes up slowly. P5 also experiences sharp variation and then decreases to a lower value. The two PPTs have their residual values $\triangle u_r$ decrease with the soil depth.

Fig. 9d shows the excess pore pressure generated inside the model bucket. Positive pore pressure instead of suction is generated, indicating that this horizontal loading leads to shear compression of the inside soil.

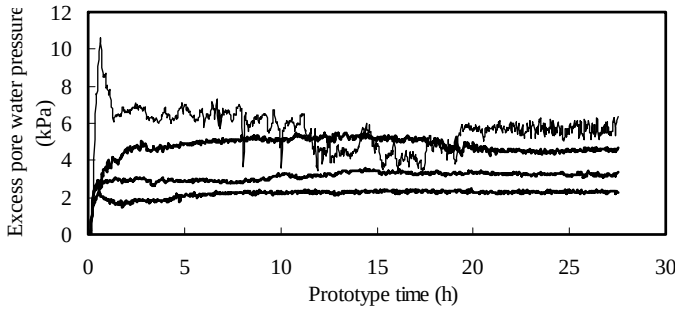

(a) Excess pore pressure of P1, P2, P3 and P4

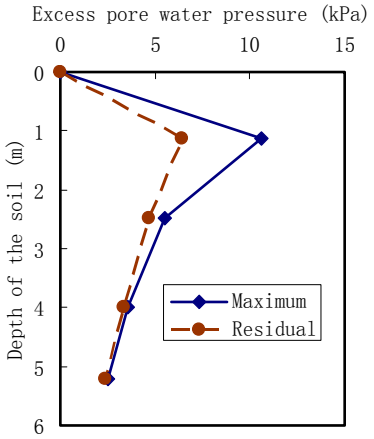

(b) Profiles of the excess pore pressure at P1, P2, P3 and P4

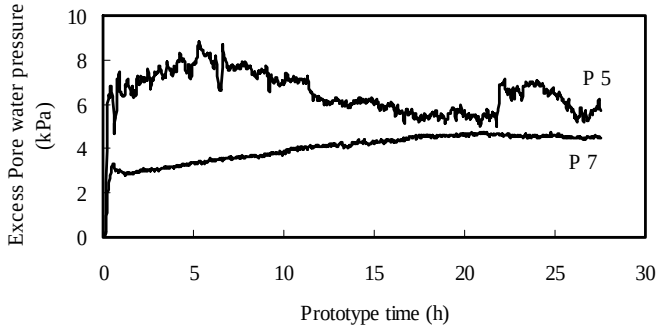

(c) Excess pore pressure of P5 and P7.

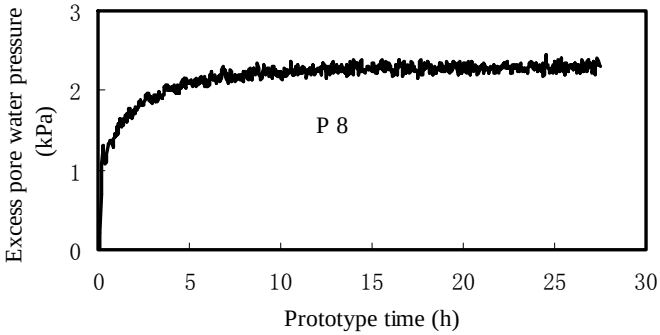

(d) Excess pore pressure of P8

Fig.9 Excess pore water pressure in Model 1.

The soil surrounding the model bucket is weakened due to the excess pore water pressure. 80 cm (in Prototype) residual settlement was observed, as shown in Fig. 10. During the excitation, 61% settlement happened within one hour, which seems associated with the occurrence of the maximum pore water pressure in the soil. Successive shaking makes the silt densification. Therefore 80% settlement was completed within 5 hours when the pore water pressures tend to be stable. Since the model bucket is connected to the actuator, so the horizontal displacement can not make sense and thus was not presented herein.

Table 4. Excess pore water pressure in the silt

PPT No.	Prototype depth of PPT (m)	Vertical effective soil stress σ_v' (kPa)	Maximum excess pore water pressure $\triangle u_m$ (kPa)	$\frac{\Delta u_m}{\sigma_v'}$	Residual excess pore water pressure $\triangle u_r$ （kPa）	$\frac{\Delta u_r}{\sigma_v'}$
P1	1.12	10.98	10.58	0.96	6.39	0.582
P2	2.48	24.3	5.53	0.23	4.68	0.193
P3	4	39.2	3.59	0.09	3.38	0.086
P4	5.2	50.96	2.48	0.049	2.35	0.046
P5	0.96	9.41	8.87	0.94	5.75	0.611
P6			Failed			
P7	4	39.2	4.8	0.12	4.51	0.115
P8	0.8	7.84	2.59	0.33	2.30	0.293

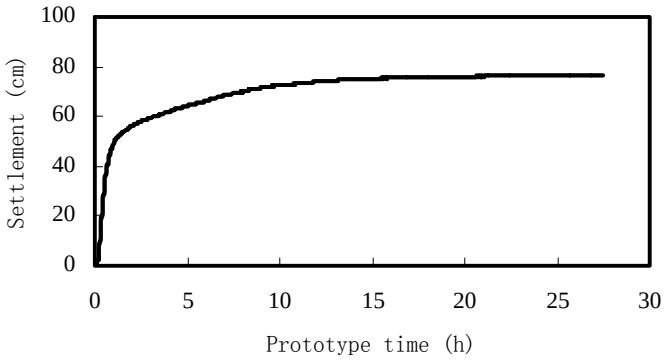

Fig. 10 Settlement of the bucket foundation

Model 2

The length of the bucket is increased to 90 mm. Fig. 11 shows the layout of eight pore water pressure transducers. P8 was placed beneath the bucket but failed in the test. The loading function is the same as Model 1.

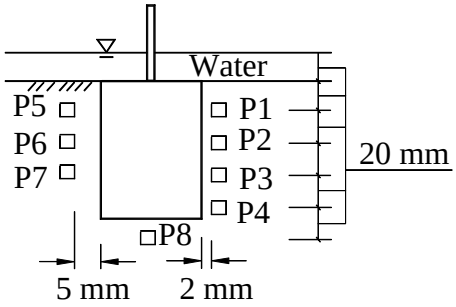

Fig. 11 Layout of the PPTs of No 1~8 for Model 2.

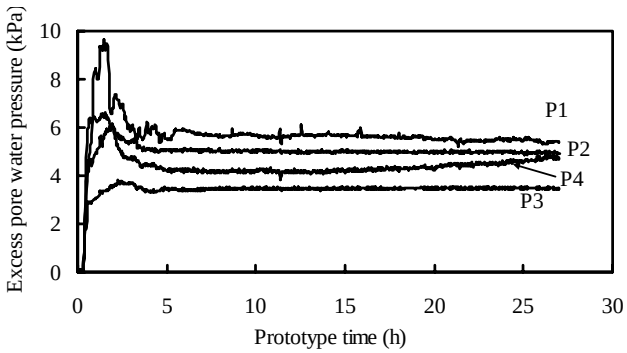

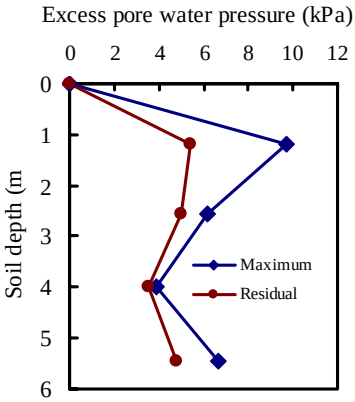

(a) P1, P2, P3 and P4

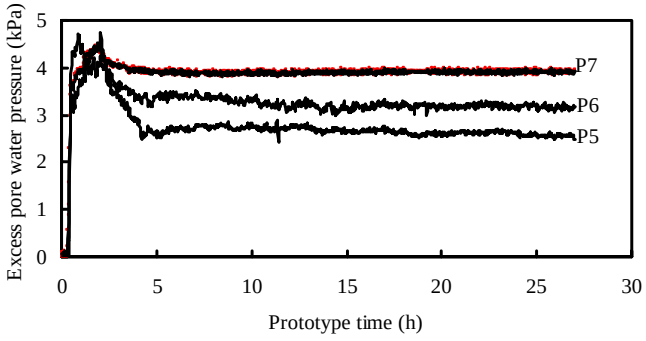

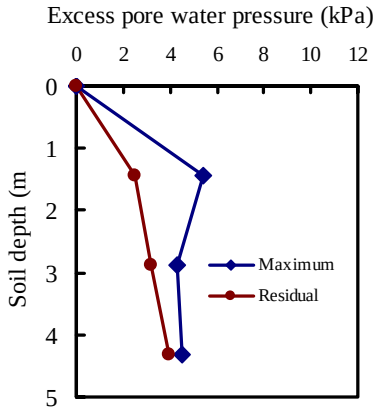

(b) P5, P6 and P7

Fig. 12 Excess pore water pressure in Model 2.

Table 5. Excess pore water pressure in the silt

PPT No.	Prototype depth of PPT (m)	Vertical effective stress σ_v' (kPa)	Maximum excess pore water pressure $\triangle u_m$ (kPa)	$\frac{\Delta u_m}{\sigma_v'}$	Residual excess pore water pressure $\triangle u_r$ （kPa）	$\frac{\Delta u_r}{\sigma_v'}$
P1	1.2	11.76	9.7	0.82	5.44	0.46
P2	2.56	25.09	6.18	0.25	4.98	0.2
P3	4	39.2	3.85	0.1	3.52	0.09
P4	5.44	53.31	6.63	0.12	4.81	0.09
P5	1.44	14.11	5.41	0.38	2.49	0.18
P6	2.88	28.22	4.33	0.156	3.16	0.11
P7	4.32	42.34	4.5	0.11	3.95	0.09
P8	7.76	76.05	Failed			

Fig. 12 shows the excess pore water pressure in Model 2 during excitations. Values in Fig. 12 are transferred to prototype scale. Fig. 12a shows the excess pore pressure recorded by P1, P2, P3 and P4, and the pressure profiles at 2 mm horizontal distance from the side of the bucket. From Fig.12a, similar character is indicated as that in Model 1. However, the ratio of maximum excess pore pressure Δu_m over the vertical effective stress σ_v' in the soil is decreased to 0.82, as shown in Table 5. High excess pore water pressure also occurs within a depth of 1.5 m. However, the profile of the pressure is different, compared to Model 1. The profile curves present the maximum pressure at P1, continuous decrease at P2 and P3, and increase at P4.

Fig. 12b shows the excess pore pressure recorded by P5, P6 and P7 PPTs, which were installed 5 mm from the side of the bucket. Although P5 was located at almost the same position, it recorded much lower pressure than P1. The bucket with a greater length acts as a deeper foundation, thus cyclic loading that transferred to the foundation soil is reduced. Therefore, these three transducers present small peak before arriving at a steady state. The profile curve of the maximum pressure appears similar to that in Fig.12a, but the residual curve presents different character.

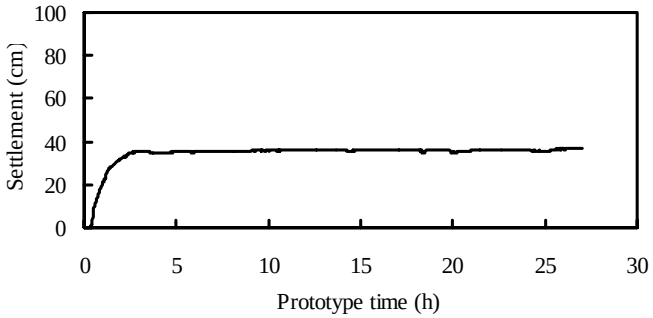

Fig. 13 Settlement of the bucket foundation

The prototype residual settlement of the bucket is 37 cm, as shown in Fig. 13. Comparing the settlement curves in Figs. 10 and 13, the settlement of the bucket in Model 2 is much lower than that in Model 1, indicating a strong effect of foundation dimensions. Furthermore, 95% settlement of Model 2 happened within three hours.

CONCLUSION

A dynamic loading device composed primarily of an electromagnetic actuator has been developed on the 50 g-t geotechnical centrifuge at Tsinghua University, by the Institute of Mechanics, China Academy of Science and Tsinghua University. Performance at 1 g and 80 g of the loading device has been presented. With this device, the amplitude and the frequency of a horizontal cyclic force is reproduced at centrifugal acceleration of 80 g.

Centrifuge test has been carried out to investigate the behavior of a suction bucket under horizontal cyclic loading for a duration of prototype 26.7 hours. From Model 1, it is indicated that excess pore water pressures were generated in the silt surrounding the bucket. The maximum excess pore water pressure is approximately equal to the vertical effective soil stress, e.g. $\Delta u_m/\sigma_v'$ ratio is 0.94~0.96. Liquefaction potential exists within a depth of 1.5 m. The residual pore water pressure decreases with the depth. Since the soil is weakened during long time excitation, great settlement was observed.

Results of Model 2 show that the length of the bucket has strong effect on the foundation response. The bucket with a greater length acts as a deeper foundation, which reduces the cyclic loading that transferred to the foundation soil. Therefore, the excess pore water pressure in the soil and the settlement of the bucket are significantly decreased. Accordingly, $\Delta u_m/\sigma_v'$ ratio falls down to 0.82.

REFERENCE

Allersma, HGB, Plenevaux, FJA, and Wintgens, JF (1997). “Simulation of Suction Pile Installation in Sand in a Geocentrifuge,” *Int J Offshore and Polar Eng*, ISOPE, Vol 3, pp 761-766.

Allersma,HGB, Kirstein,AARB, and Brinkgreve,TS (1999). “Centrifuge and Numerical Modeling of Horizontally Loaded Suction Piles.” *Int.J Offshore and Polar Eng*,ISOPE.Vol1.pp 711-717.

Allersma, HGB, Hogervosrst, JR, and Pimoulle, M (2001). “Centrifuge Modeling of Suction Pile Installation in Layered Soil by Percussion Method.” *OMAE Conf.* Vol1, pp 87-93.

Allersma, HGB, and Jacobse, JA (2003). "Centrifuge Tests on Pullout Capacity of Suction Caissons with Active Suction." *13th International Conference on Offshore and Polar Engineering* (ISOPE03), Honolulu, May 25-30.

Cao, JC (2003). Centrifuge modeling and numerical analysis of the behavior of suction caissons in clay. *Ph.D. Thesis.* Memorial University of Newfoundland. St. John's Newfoundland, Canada.

Clukey, EC, and Morrison, MJ (1993). "A Centrifuge and Analytical Study to Evaluate Suction Caissons for TLP Application in the Gulf pf Mexico." *Proc. ASCE Conference on Foundations*, Dallas, TX. Vol 1, pp 141-156.

Clukey, EC, and Morrison, MJ (1995). "The Response of Suction Caissons in Normally Consolidated Clays to Cyclic TLP Loading Conditions." *Offshore Technology Conference* OTC7796. Vol 3, pp 909-915.

Craig, WH (1981). "Cyclic Loading Equipment for Offshore Foundation Model". *Offshore Structures: The Use of Physical Models in Their Design*, eds. Armer, G.S.T. and Garas, F.K. 327-334. Construction Press. NY.

Dean, ETR, Hsu,YS, and Schofield,AN (1993). "Development of a New Apparatus for Centrifuge Testing of Offshore Jackup Platform Models and Data Report for Centrifuge Test YSH1: 3-leg Jackup Model with Flat Spuds on Dense Watwe-saturated Sand". *Technical Report CUED/D-Soils/TR267*. University of Cambridge, London.

Fuglsang LD, Steensen-Bach, JO(1991). "Breakout Resistance of Suction Piles in Clay". *Centrifuge 91*, H. Y. Ko &F. G. Mclean(ed.), Balkema, Rotterdam, 1991, pp 153-159

Hjortnaes-Pedersen, AG and Nelissen, HAM (1991). "Application of Hydraulic Actuators in The Delft Geotechnical Centrifuge." *Centrifuge 91*. Ko, HY & Mclean, F G (ed.), Balkema, Rotterdam. pp 385-390.

Kutter, BL. and James, RG (1989). "Dynamic Centrifuge Model Tests on Clay Embankments,". *Geotechnique* Vol 39, No.1, pp 91-106.

Lee, FH, and Scholfield, AN (1988). "Centrifuge Modeling of Sand Embankments and Islands in Earthquake," *Geotechnique* Vol 38, No. 1, pp 45-58.

Ng, TG, Lee, FH, Liaw, CY and Chan, ES (1994). "Development of a Dynamic Loading Device for Model Foundation". *Proc. of Int. Conference Centrifuge 94*, Singapore/31 Aug.-2 Sept., Vol 1, pp 183-188.

Pu, JL, Liu, FD, Li, JK, Li, SQ, Yin, KT, Sun, YS, and Jin, PF (1994). "Development of Medium-size Geotechnical Centrifuge at Tsinghua University." *Proc. of Int. Conference Centrifuge 94*, Singapore/31 Aug.-2 Sept., Vol 1, pp 53-56.

Renzi, R, Maggioni, W, and Smith, F (1991). "A Centrifugal Study on the Behavior of Suction Piles." *Centrifuge 91*, H. Y. Ko &F. G. Mclean(ed.), Balkema, Rotterdam, Vol 1, pp 169-176.

Tan, FSC (1990). Centrifuge and theoretical modeling of conical footings on sand. *Ph.D. Thesis*, Cambridge University, Jan, 1990.

Waston, PG, and Randolph, MF (1997). "Vertical Capacity of Caisson Foundations in Calcareous Sediments," *Proceedings of the seventh International Offshore and Polar Engineering Conference*, Honolulu, USA, May 25-30, pp 784-790.

Zhang, JH, Yan, D, Sun, GL, and Li, WX (2003). "Development of a Dynamic Loading Device for Suction Pile in Centrifuge," BGA *International Conference on foundations: "Innovations, Observations, Design and Practice"* 2nd-5th Sep. University of Dundee, Scotland, Vol 1, pp 985-990.